Enhanced catalytic activity, optical, magnetic and anti-bacterial studies of pure and Ni-doped ZnO nano-particles

V. Sumithra [1], B. Anthea[1], M. R. Ranjani [1], N. Ramalakshmi [1], S. Arul Antony [1*]

[1]PG & Research Department of Chemistry, Presidency College (Autonomous), Chennai - 600 005, Tamil Nadu, India

ABSTRACT

In this paper, pure and transition element (Nickel) doped ZnO nanoparticles were synthesized via simple wet-chemical technique at low temperature. The structural studies carried out by XRD and it is reveal that the synthesized nanoparticles were well-crystalline and possessing hexagonal wurtzite structure. HR-SEM images depicted the homogenous spherical shaped ZnO nanoparticles. UV-Visible absorption spectra showed that the optical band gap value of pure ZnO increased by Ni doping. PL spectra confirmed that the effective Ni doping enhances the visible emission and suppresses the near band gap emission. The presence of functional groups was ensuring by FT-IR spectroscopy studies. The bactericidal efficiency of Ni doped ZnO nanoparticles were investigated against a Gram positive (Bacillus subtilis, Staphylococcus aureus) and Gram negative bacteria (Proteus mirabilis, Salmonella typhi). The effect of Ni doping on the photocatalytic activity of ZnO nanoparticles for the degradation of methylene blue (MB) dye was studied under solar illumination and the results showed that the Ni doping kindles appreciable degradation of MB.

Keywords: ***Ni doped ZnO; Nanoparticles; Chemical method; FT-IR spectroscopy; Antibacterial activity.***

1. Introduction

Recently, semiconductor nanomaterials with larger surface area have attracted much attention, because of their fundamental research application in various fields, due to unique size and shape dependent optical, electrical, magnetic, photocatalytic, biomedical properties [1-10]. Such metal oxide semiconducting nanomaterials TiO_2, SnO_2, MgO, V_2O_5 and AgO are used, due to their vast emitting as well as potential application, especially as biocides or disinfecting agents [11-15]. Among these oxide, ZnO nanomaterials with hexagonal wurtzite structure is well known n-type (II-IV) semiconductor with a wide band gap of (3.37 eV) and large exition binding energy of 60 meV [16-20]. Owing to these unique properties, ZnO

nanomaterials are exhibiting versatile applications in various [21]. However its preparation is ever developed and a suitable method for preparing ZnO possessing low cost, less time, easy to prepare, working at ambient temperature. For the moment, doping in ZnO alter the optical, electrical, catalytic and magnetic properties [22-25]. Among the other transition element dopants ions Ni^{2+} ions easy incorporation into ZnO crystal and enhances their potential applications [26]. However, very few papers have been reported on the catalytic and biological application of Ni doped ZnO nanoparticles. Inspired by these investigations, in this work, Ni doped ZnO nanoparticles were synthesized by eco-friendly wet-chemical method, which is a simple, easy to handle, very effective but inexpensive method [27]. Furthermore, the emphasis on antibacterial activities of the synthesized pure and Ni doped ZnO nanoparticles were tested against gram positive (Bacillus subtilis, Staphylococcus aureus) and gram negative (Proteus mirabilis, Salmonella typhi) bacterial strains and results were compared against the standard antibiotic ampicillin.

Among the diverse applications of ZnO nanostructures in multidisciplinary areas, photocatalysis is the most important one for the environmental security. In addition, it is well known that ZnO exhibit the different morphologies. It is well known that the metal dopants have also been used to recover the morphology and enhanced photocatalytic activity. When metal was doped into ZnO lattice, more surface defects are twisted, which delayed the recombination of photo-induced electron–hole pairs, which contribute to the enhancement of the photocatalytic activity. Hence, the authors have investigated the connection among photocatalytic activity, particle size, and morphology of ZnO particles in detail. In addition, the influence of Ni-dopants on structure, morphology, optical, magnetic and photocatalytic activity of ZnO nanoparticles was investigated thoroughly in the present study.

2. Materials and Methods

2.1. Preparation of Ni-doped ZnO nanoparticles

The zinc acetate (0.1 M) was prepared in 100 mL methanol at room temperature and 1 mL of octylamine was introduced into the solution which controls the growth of nucleation. The above solution was continuously stirred for 24 h for gently homogenous solution. Then, 0.05 moles of nickel nitrate was added into the above precursor solutions. Finally, 3 M NaOH was slowly added drop wise into the solution until pH attains 12. The solution was aged about 1h and the precipitates were collected out for washing water to remove the unreacted reagents. The slurry was dried in an oven at 80 ˚C for about 10 h was annealed at 400 ˚C for 2 h. The pure ZnO sample was prepared by adopting the same procedure without adding manganese nitrate.

2.2. Characterization

X-ray diffraction (XRD) pattern was recorded at room temperature using (PAN analytical X'Pert PRO equipment using CuKα irradiation as found wavelength (λ= 1.5418 Å). The morphology and elemental composition analysis of the sample was investigated by High resolution scanning electron microscope using (JEOL, JSM-67001). The optical absorption spectra were recorded by UV-Vis absorption spectrometer (Perkin Elmer T90 + Spectrophotometer). Room-temperature photoluminescence [PL] spectral measurements were carried out using JY Fluorolog-3-11 spectrometer. The solid phase FT-IR spectrum in KBr pellet technique was recorded with (FT-IR; JASCO, Model 6300).

2.3. Antibacterial activity

Antimicrobial activity was tested in both gram-negative and gram-positive bacteria namely *Staphylococcus aureus*, *Proteus mirabilis*, S*almonella typhii* and *Bacillus subtilis* by disc diffusion method with small modifications. The 24 h bacterial cultures were swabbed in a Muller Hinton agar (MHA) amended plates. Whatmann filter paper (No.1) discs of 3 mm

diameter were impregnated with 100 µL of the solution containing samples (ZnO and $Mn_{0.5}Zn_{0.5}O$) and these discs were allow to evaporation for 1 h. Reference standard discs were prepared with ampicillin (10 µg/mL) to compare the antibacterial activity of the samples. After drying, the discs were placed in swabbed bacterial plates and incubated at 28 °C for 24 h. After incubation, plates were examined for clear zone around the discs. A clear zone more than 2 mm in diameter was taken for antibacterial activity. All the experiments were carried out in triplicate and the inhibition zones of the samples were compared.

2.4. Photocatalytic reactor setup and degradation procedure

Photocatalytic degradation experiments were carried out in a self-designed photocatalytic reactor. The cylindrical photocatalytic reactor tube was made up of quartz/borosilicate with a dimension of 36–1.6 cm (height-diameter). The top portion of the reactor tube has ports for sampling, gas purging, and gas outlet. The aqueous methylene blue solution containing appropriate quantity of either pure ZnO or Ni-doped ZnO was taken in the quartz/borosilicate tube and subjected to aeration for thorough mixing. This was then placed inside the reactor setup. The lamp housing has low pressure mercury lamps emitting either 254 or 365 nm with polished anodized aluminum reflectors and black cover to prevent UV leakage. The PCD was carried out by mixing 100 mL of aqueous methylene blue solution and fixed weight of pure ZnO or Ni-doped ZnO photocatalysts.

3. Results and discussion

3.1. Structural studies

Powder X-ray diffraction analysis was used to investigate the crystal structure and phase purity of pure and Ni doped ZnO Nanoparticles. Figure 1 compares the XRD pattern of pure and nickel doped ZnO. The diffraction peaks observed for the crystal planes (100), (002) and (101) at 2θ = 32.5°, 34.3º, 36.2º confirmed the wurtzite hexagonal ZnO crystalline planes of JCPDS No: 34-1451 [28]. The sharp diffraction peaks in the XRD patterns explain that

ZnO is highly crystalline in nature. It is observed that the broadening of XRD peak of Ni doped samples that reduce the size of ZnO nanoparticles [29]. The average crystallite size was estimated by using Scherrer formula.

$$D = K\lambda / \beta \cos\theta \quad (1)$$

Where, K is a shape constant (0.89), λ is the wavelength of X-ray (0.1540 nm), β is the full width at half maximum and θ is the angle of diffraction. From the d spacing values, lattice constant 'a' and 'c' can be calculated by using the Equation (1) and their values are presented in Table 1 along with particle size.

$$1/d^2 = 4/3(h^2+hk+k^2/a^2) + l^2/c^2 \quad (8)$$

The calculated aspect ratio of pure and Ni-doped ZnO is in good agreement with the reported value of 1.60 of ZnO. It confirms that the Ni^{2+} is substituted Zn^{2+} ions in the overall crystal structure [30].

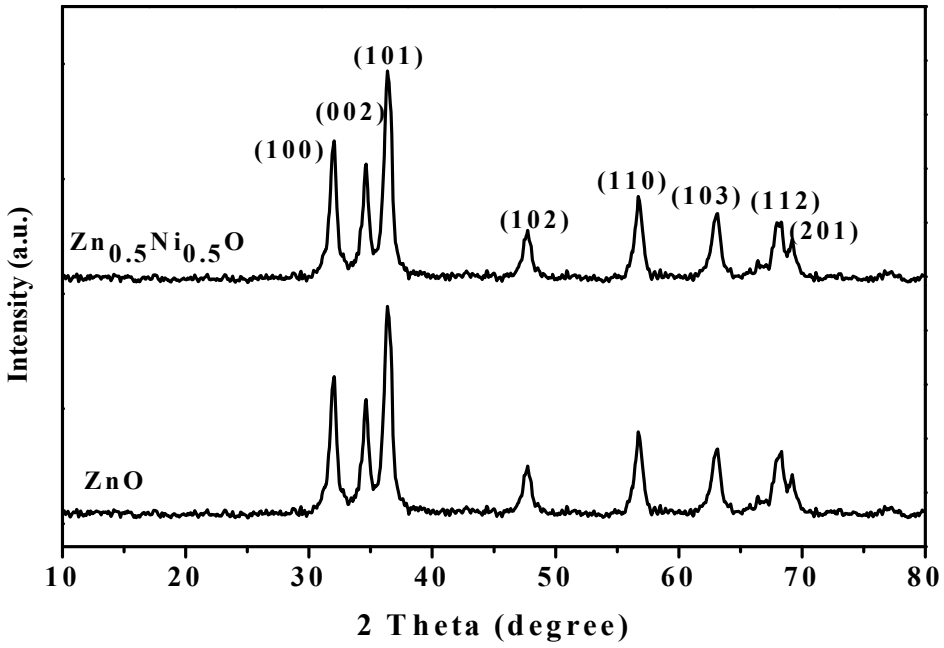

Figure 1. Powder XRD pattern of pure and Ni doped ZnO Nanoparticles

Table1. Structural parameters of pure and Ni doped ZnO nanoparticles.

Sl.No.	Samples	Lattice parameter values (Å)			Crystallite size, D (nm)	Volume (V) $(Å)^3$
		(a)	(c)	c/a		
1.	ZnO	3.245	5.204	1.604	34.68	49.15
2.	$Zn_{0.5}Nin_{0.5}O$	3.237	5.187	1.601	29.30	48.44

3.2 FT-IR studies

FT-IR spectra of pure and Ni doped ZnO nanoparticles recorded at room temperature in the range of 400 cm^{-1} – 4000 cm^{-1} are presented in Figure 2. A broad band occurred at 3200-3400 cm^{-1} is due to the stretching mode of O–H group that tells the existence of water content in the sample [31]. Few peaks at below 950 -400 cm^{-1} is due to the metal – oxygen bands (Ni-O, Zn-O and Zn-O-Ni) [32].

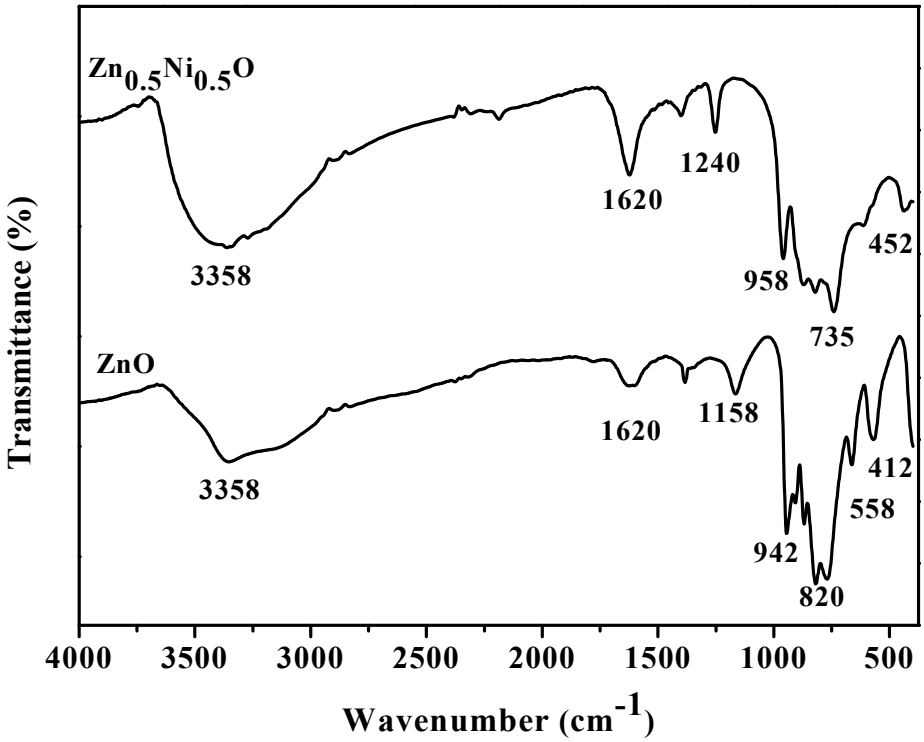

Figure 2. FTIR spectra of pure and Ni doped ZnO Nanoparticles

3.3. HR-SEM/EDX studies

HR-SEM images of pure and Ni doped ZnO Nanoparticles are shown in Figure 3 (a,b). From the images, it is noticed that both the samples consists uniform spherical ZnO nanoparticles. There were no agglomerations between the particles observed. It is well-known that the strongly adsorbed stabilizer prevents the aggregation between the particles due to its steric hindrance effect [33].

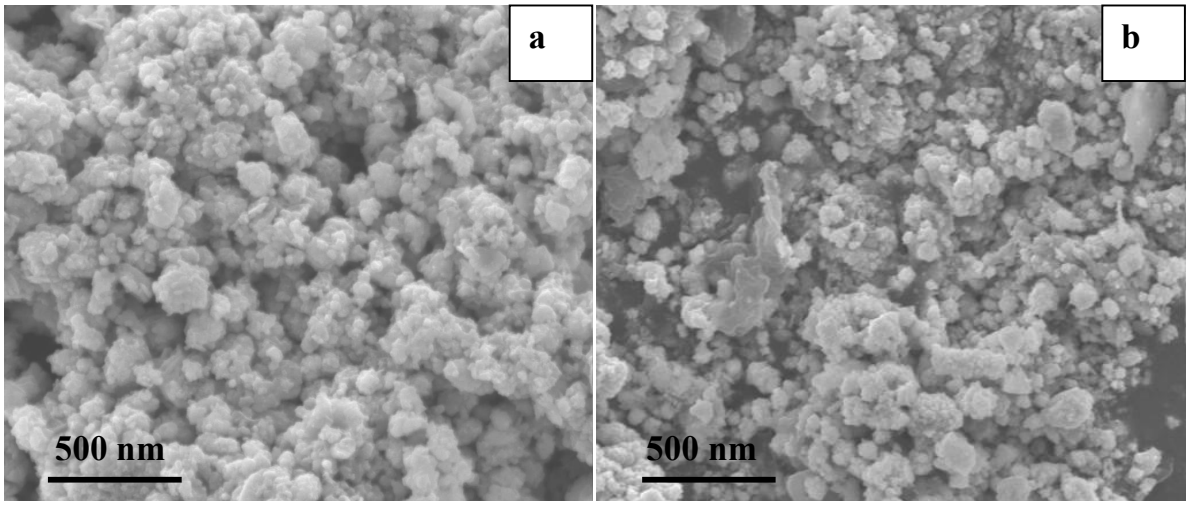

Figure 3. HR-SEM images of pure (a) and Ni doped ZnO (b) nanoparticles

3.4. UV-Vis spectral studies

UV-Vis spectra of pure and Ni doped ZnO nanoparticles were recorded using UV-Vis spectrophotometer in the wavelength range 200 - 800 nm at room temperature and absorbance spectra are shown in Figure 4. It is clearly indicates that the Ni-dopant in the ZnO lattice. Such localized electronic states have also been reported to form the new unoccupied molecular orbitals and facilitate the band gap reduction of host compound [34]. As a result, average atomic distance increases and then the band gap could be decreased. Hence, the turnable narrowing energy gap by doping of Ni into ZnO sample will be suitable for promising photonic device application and UV-Vis light photocatalysts.

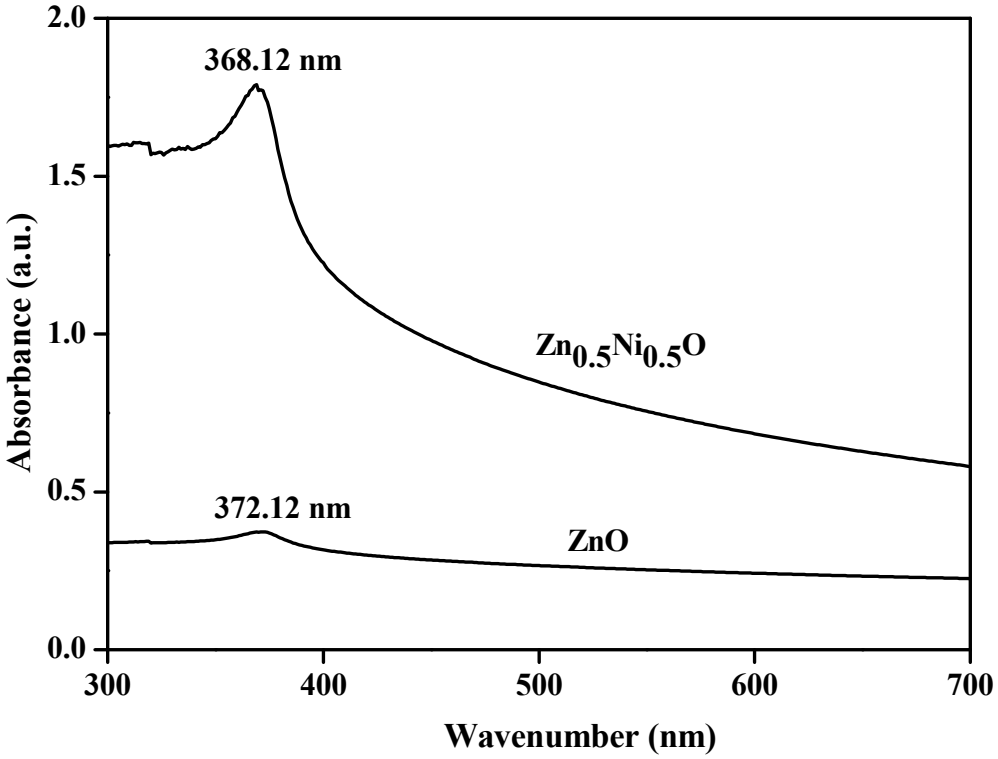

Figure 4. UV-Vis spectrum of pure and Ni doped ZnO Nanoparticles

3.5. Photoluminescence (PL) studies

PL spectra recorded at room temperature for pure and Ni doped ZnO nanoparticles by exciting radiation of 325 nm as shown in Figure 5. PL spectra shown a number of peaks in the range 415-530 nm. A peak observed at 415 nm is attributed to near band edge (NBE), due to the defect states in the Ni doped ZnO nanoparticles. The appearance of emission band at 448 nm is attributed to the transition from Zn interstitial to valence bands (VB), where as the emissions at 476,d 496 and 530 nm, most probably from the oxygen vacancies [35]. These results demonstrate a great promise for narrow band gap Ni doped ZnO nanoparticles with potential applications in optoelectronic devices.

Figure 5 PL spectrum of pure and Ni doped ZnO Nanoparticles

3.6 Photocatalytic degradation

Commonly, ZnO semiconductor nanoparticles have been expansively studied as one of the probable photo-catalyst. In this present study, photocatalytic activity for the degradation of methylene blue (MB) dye was carried out in aqueous suspension (Fig. 6). A control experiment was carried out in the absence of the samples by irradiating the solution with UV radiation (photolysis) and found that the photo-catalytic degradation efficiency lesser than 10%. But, the photo-catalytic degradation efficiency of ZnO is lower than that of Ni-doped ZnO due to the difference in the crystallite size, shape, and surface morphology of the samples [36].

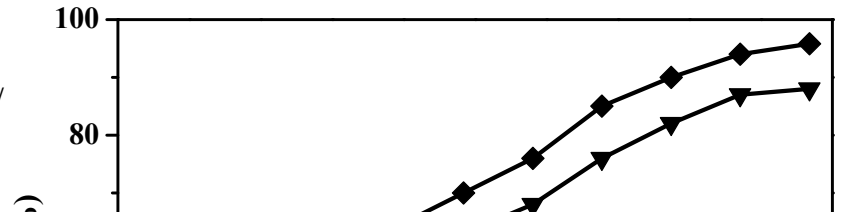

Figure 6. Photo-catalytic degaradation activity of pure and Ni doped ZnO nanoparticles

3.7. Antibacterial activity

Generally, ZnO nanoparticles are well known investigated potential semiconductor for photocatalysis, sensing and antimicrobial application. In this present study, antibacterial activity of pure and Ni-doped ZnO suspension of particles towards gram positive and gram negative were studied. It was observed that the antibacterial activity increased with the increasing Ni dopant in ZnO lattice and the inhibition of *P. mirabilis* is slightly larger than other bacteria, which may due to the difference in structure and chemical composition of the cell surface [37]. Furthermore, it is clear that the antibacterial activity increased with decrease in particle size. Pure ZnO possesses less antibacterial activity, while $Zn_{0.5}Ni_{0.5}O$ possesses higher antibacterial activity related to standard ampicillin (Table 2). From the antibacterial

test, it is confirmed that Ni doped ZnO nanoparticles render an effective antibacterial agent, when compared to pure ZnO.

Table 2. Antibacterial activity of pure and Ni doped ZnO nanoparticles against human pathogens

Antibacterial activities of samples were determined as zone of inhibition (in mm)				
Samples	***P. mirabilis***	***S .typhi***	***S. aureus***	***B. subtilis***
Ampicillin (C)	24	19	12	11
ZnO	8	5	1	1
$Zn_{0.5}Ni_{0.5}O$	23	8	0	1

4. Conclusion

Pure and Ni doped ZnO nanoparticles were synthesised via chemical method. Powder XRD pattern exhibited wurtzite structure. Spherical morphology was found for pure and Ni doped ZnO nanoparticles by HR-SEM images. Pho to-catalytic analysis was further confirmed the catalytic degradation efficiency of pure and Ni doped ZnO nanoparticles and found that Ni-doped ZnO which is slightly higher activity than pure ZnO. So that it proved to be the incorporation of Ni ions in ZnO lattice, which enhanced the PCD activity. Antibacterial studies against gram positive and gram negative bacterial strains on pure and Ni doped ZnO confirmed that Ni doped ZnO nanoparticles possess an enhanced antibacterial effect than pure ZnO, due to the smaller particle size with higher surface area.

References

[1] A. P. Subramanian, S. K. Jaganathan, A. Manikandan, K. N. Pandiaraj, N. Gomathi and E. Supriyanto, RSC Adv., 6 (2016) 48294-48314.

[2] V.Muthuvignesh, V.J. Reddy, S. Ramakrishna, S. Ray, A.Ismail, M.Mandal, A. Manikandan, S. Seal and S. K. Jaganathan, RSC Adv., 6 (2016) 83638-83655.

[3] V. Muthuvignesh, S. K. Jaganathan, A. Manikandan, RSC Adv., 6 (2016) 114859-114878.

[4] G. Padmapriya, A. Manikandan, V. Krishnasamy, S. K. Jaganathan, S. Arul Antony, Journal of Molecular Structure, 1119 (2016) 39-47.

[5] V. Mary Teresita, A. Manikandan, B. Avila Josephine, S. Sujatha, S. Arul Antony, J. Supercond. Nov. Magn., 29 (2016) 1691–1701.

[6] S. Jayasree, A. Manikandan, S. Arul Antony, A. M. Uduman Mohideen, C. Barathiraja, J. Supercond. Nov. Magn., 29 (2016) 253–263.

[7] C. Barathiraja, A. Manikandan, A. M. Uduman Mohideen, S. Jayasree, S. Arul Antony, J. Supercond. Nov. Magn., 29 (2016) 477-486.

[8] B. Avila Josephine, A. Manikandan, V. Mary Teresita, S. Arul Antony, Korean J. Chem. Eng., 33 (2016) 1590-1598.

[9] A. Manikandan, M. Durka, M. A. Selvi, S. Arul Antony, J. Nanosci. Nanotech., 16 (2016) 448-456.

[10] A. Manikandan, M. Durka, M. A. Selvi, S. Arul Antony, J. Nanosci. Nanotech., 16 (2016) 357-373.

[11] A. Manikandan, R. Sridhar, S. Arul Antony, S. Ramakrishna, J. Mol. Struct., 1076 (2014) 188-200.

[12] A. Manikandan, M. Durka, S. Arul Antony, J. Supercond. Nov. Magn., 27 (2014) 2841–2857.

[13] A. Manikandan, S. Arul Antony, J. Supercond. Nov. Magn., 27 (2014) 2725-2733.

[14] A. Manikandan, M. Durka, S. Arul Antony, J. Inorg. Organomet. Polym. 25 (2015) 1019–1031.

[15] A. Manikandan, M. Durka, K. Seevakan, S. Arul Antony, J. Supercond. Nov. Magn., 28 (2015) 1405-1416.

[16] A. Manikandan, M. Durka, S. Arul Antony, J. Supercond. Nov. Magn., 28 (2015) 209–218.

[17] A. Manikandan, E. Hema, M. Durka, M. Amutha Selvi, T. Alagesan, S. Arul Antony, J. Inorg. Organomet. Polym. 25 (2015) 804–815.

[18] A. Manikandan, E. Hema, M. Durka, K. Seevakan, T. Alagesan, S. Arul Antony, J. Supercond. Nov. Magn., 28 (2015) 1783-1795.

[19] A. Manikandan, M. Durka, S. Arul Antony, J. Supercond. Nov. Magn., 28 (2015) 2047–2058.

[20] K. Chinnaraj, A. Manikandan, P. Ramu, S. Arul Antony, P. Neeraja, J. Supercond. Nov. Magn., 28 (2015) 179-190.

[21] E. Hema, A. Manikandan, P.Karthika, M. Durka, S. Arul Antony, B. R. Venkatraman, J. Supercond. Nov. Magn., 28 (2015) 2539-2552.

[22] D. K. Manimegalai, A. Manikandan, S. Moortheswaran, S. Arul Antony, J. Supercond. Nov. Magn., 28 (2015) 2755-2766.

[23] V. Umapathy, A. Manikandan, S. Arul Antony, P. Ramu, P. Neeraja, Transactions of Nonferrous Metals Society of China, 25 (2015) 3271-3278.

[24] A. Manikandan, S. Arul Antony, R. Sridhar, Seeram Ramakrishna, M. Bououdina, J. Nanosci. Nanotech., 15 (2015) 4948-4960.

[25] A. Manikandan, M. Durka, S. Arul Antony, Adv. Sci. Eng. Med., 7 (2015) 33-46.

[26] A. Manikandan, A. Saravanan, S. Arul Antony, M. Bououdina, J. Nanosci. Nanotech., 15 (2015) 4358-4366.

[27] M. F. Valan, A. Manikandan, S. Arul Antony, J. Nanosci. Nanotech., 15 (2015) 4580-4586. (IF: 1.483).

[28] M. F. Valan, A. Manikandan, S. Arul Antony, J. Nanosci. Nanotech., 15 (2015) 4543-4551.

[29] K. Chitra, K. Reena, A. Manikandan, S. Arul Antony, J. Nanosci. Nanotech., 15 (2015) 4984-4991.

[30] S. Jayasree, A. Manikandan, A. M. Uduman Mohideen, C. Barathiraja, S. Arul Antony, Adv. Sci. Eng. Med., 7, (2015) 672-682.

[31] K. Chitra, A. Manikandan, S. Moortheswaran, K. Reena, S. Arul Antony, Adv. Sci. Eng. Med., 7 (2015) 710-716.

[32] D. K. Manimegalai, A. Manikandan, S. Moortheswaran, S. Arul Antony, Adv. Sci. Eng. Med., 7, (2015) 722-727.

[33] A. Mary Jacintha, A. Manikandan, K. Chinnaraj, S. Arul Antony, P. Neeraja, J. Nanosci. Nanotech., 15 (2015) 9732-9740.

[34] K. Reena, R. Gunaseelan, A. Manikandan, S. Arul Antony, Adv. Sci. Eng. Med., 8 (2016) 245-249.

[35] S. Moortheswaran, A. Manikandan, S. Sujatha, S. K. Jaganathan, S. Arul Antony, Nanosci. Nanotech. Lett., 8 (2016) 434-437.

[36] B. Meenatchi, K. R. N. Deve, A. Manikandan, V. Renuga, and V. Sathiyalakshmi, Adv. Sci. Eng. Med., 8 (2016) 653-659.

[37] K. Chitra, A. Manikandan, S. Arul Antony, J. Nanosci. Nanotech., 16 (2016) 758-764.